1 Fluctuating pH for efficient photomixotrophic succinate production

- 2 Tanner R Treece¹, Marissa Tessman², Robert S. Pomeroy³, Stephen P. Mayfield^{4,5},
- 3 Ryan Simkovsky^{4,5} and Shota Atsumi^{1,*}
- ¹Department of Chemistry, University of California, Davis, Davis, CA, 95616, USA
- ⁵ Algenesis Inc.,1238 Sea Village Dr., Cardiff, CA, USA
- ³Department of Chemistry and Biochemistry, University of California, San Diego, La
- 7 Jolla, CA, 92093, USA
- ⁴Division of Biological Sciences, University of California, San Diego, La Jolla, CA,
- 9 92093, USA

- ⁵California Center for Algae Biotechnology, University of California, San Diego, La Jolla,
- 11 CA, 92093, USA
- *To whom correspondence may be addressed: E-mail: satsumi@ucdavis.edu

Abstract

14

15

16

17

18

19

20

21

22

23

24

25

26

27

28

29

30

31

32

33

34

35

Cyanobacteria are attracting increasing attention as a photosynthetic chassis organism for diverse biochemical production, however, photoautotrophic production remains inefficient. Photomixotrophy, a method where sugar is used to supplement baseline autotrophic metabolism in photosynthetic hosts, is becoming increasingly popular for enhancing sustainable bioproduction with multiple input energy streams. In this study, the commercially relevant diacid, succinate, was produced photomixotrophically. Succinate is an important industrial chemical that can be used for the production of a wide array of products, from pharmaceuticals to biopolymers. In this system, the substrate, glucose, is transported by a proton symporter and the product, succinate, is hypothesized to be transported by another proton symporter, but in the opposite direction. Thus, low pH is required for the import of glucose and high pH is required for the export of succinate. Succinate production was initiated in a pH 7 medium containing bicarbonate. Glucose was efficiently imported at around neutral pH. Utilization of bicarbonate by CO₂ fixation raised the pH of the medium. As succinate, a diacid, was produced, the pH of the medium dropped. By repeating this cycle with additional pH adjustment, those contradictory requirements for transport were overcome. pH affects a variety of biological factors and by cycling from high pH to neutral pH processes such as CO₂ fixation rates and CO₂ solubility can vary. In this study the engineered strains produced succinate during fluctuating pH conditions, achieving a titer of 5.0 g L⁻¹ after 10 days under shake flask conditions. These results demonstrate the potential for photomixotrophic production as a viable option for the large-scale production of succinate.

1. Introduction

Despite efforts towards carbon remediation, atmospheric CO_2 levels continue to rise, in large part due to the current petroleum-based economy (Uprety et al., 2019). Many studies envisage that chemical commodities directly derived from biomass will play a large role in converting our petroleum-based industries to a more sustainable production platform (Cozier, 2014; Sheldon, 2014). Photoautotrophic production of chemical commodities is an important aspect of a biobased economy. Improving technologies to directly convert CO_2 towards industrially relevant titers of chemical commodities would be a boon to sustainability efforts globally. Photomixotrophy is a strategy that can be leveraged to improve production from CO_2 to chemicals in photosynthetic hosts by supplementing photoautotrophic metabolism with carbohydrate substrates sourced from waste biomass. Engineered organisms tend to leverage decarboxylation steps to produce chemical targets, therefore developing carbon conserving pathways towards these chemical products is of great interest (François et al., 2020). Using a photosynthetic bacterium allows for a carbon efficient chemical production route by harnessing the naturally occurring CO_2 fixation process to incorporate CO_2 into the chemical of interest (Kanno et al., 2017; Stephens et al., 2021).

Succinic acid or succinate, has a large market today, valued at 223 million USD in 2021 (Newark, 2020). Succinate has a wide range of applications from pharmaceuticals to bioplastic production. Commercialization of biologically-derived succinate, produced through microbial fermentation of biologically-sourced sugars, has been implemented by many companies such as Corbion, BASF, Roquette, and BioAmber. Succinate based bioplastics in particular can replace several everyday products, which can further decrease our carbon footprint by replacing polymer-based products that are difficult to recycle. Several bio-based platforms have been used to generate succinate industrially, including using heterotrophic organisms capable of high natural production, such as *Mannheimia succiniciproducens*, or engineering traditional model organisms, such as *Escherichia coli*.

Photoautotrophic production of succinate has been accomplished in recent studies focusing on engineering various cyanobacteria (Lan and Wei, 2016; Sengupta et al., 2020). The

64 TCA cycle in most cyanobacteria is bisected into two branches because these organisms are missing key enzymes to produce succinate from α -ketoglutarate and complete the cycle 65 (Steinhauser et al., 2012). The cyanobacterium Synechococcus elongatus PCC 7002 (hereafter, 66 67 7002) possesses a unique pathway for succinate production via a succinate semialdehyde 68 intermediate (Steinhauser et al., 2012). Recent studies have established that other species of cyanobacteria can produce succinate when equipped with the succinate semialdehyde pathway 69 70 from 7002 (Lan and Wei, 2016; Sengupta et al., 2020). This pathway includes two key steps, an oxoglutarate decarboxylase and a succinate semialdehyde dehydrogenase (Steinhauser et al., 71 2012). These two enzymes alone are not sufficient for significant production of succinate and 72 these engineered strains are further equipped with upstream modifications including 73 74 overexpression of the genes encoding for a phosphoenol pyruvate carboxylase and a citrate 75 synthase to enhance carbon flux into the TCA cycle (Lan and Wei, 2016; Sengupta et al., 2020). However, photoautotrophic production rates and yields of succinate significantly lag behind 76 77 heterotrophic systems (Ahn et al., 2016; Lee et al., 2011). The cyanobacterium Synechocystis sp. PCC 6803 (6803) is naturally capable of succinate production under nutrient limiting and dark 78 79 anoxic conditions through auto-fermentation, wherein intracellular glycogen is catabolized to 80 produce necessary cellular energy requirements. One study using this strategy was able to 81 achieve a titer of 1.8 g L⁻¹ succinate after 72 hours under dark anaerobic and high biomass 82 conditions (25g DCW L⁻¹) (Hasunuma et al., 2018). Another recent study further improved succinate production in 6803 and achieved a titer of 4.2 g L⁻¹ (lijima et al., 2021). One study in 83 7942 achieved a cumulative titer of 8.9 g L⁻¹ succinate photoautotrophically after 112 days 84 when using CRISPR inhibition to knockdown the activities of sdhB and qlqC (Lai et al., 2022). 85 While these studies show potential as a means to convert CO₂ into succinate, auto-86 87 fermentation requires multiple cultivation steps, anoxic conditions are often difficult to successfully implement and long production periods can be difficult to monitor. Additionally, 88 89 heterotrophic organisms still outpace photoautotrophic organisms; one study using an engineered E. coli produced ~12 g L⁻¹ succinate with a productivity of 0.17 g L⁻¹ h⁻¹ 90 heterotrophically in minimum media under shake flask conditions (Li et al., 2017). 91

In a previous study, the model cyanobacterium, *Synechococcus elongatus* PCC 7942 (hereafter, 7942), was engineered to consume glucose resulting in a photomixotrophic strain (Kanno et al., 2017). Notably, this strain was able to continue carbon fixation and chemical production during dark conditions, providing a significant milestone in the efforts to make a commercially viable microbe that can directly convert CO₂ into valuable chemicals (Berla et al., 2013; Kanno et al., 2017; Nozzi et al., 2013). Ideally, the photomixotrophic strains would be utilizing glucose from lignocellulosic hydrolysate, a strategy which allows for enhanced chemical production without competing against food supply and provides a route for recycling biomass that would otherwise be burned as waste.

This work demonstrates that photomixotrophy can be applied to enhance succinate production in cyanobacteria. The glucose utilization (Kanno et al., 2017) and succinate production (Lan and Wei, 2016) pathways were introduced into 7942. Additionally, the Calvin-Benson (CB) cycle was deregulated by removing *cp12* encoding for the CB regulatory protein Cp12, which was previously shown to improve photomixotrophic production of chemicals (Kanno et al., 2017). The gene *sdhB*, which encodes for succinate dehydrogenase subunit B was deleted to prevent conversion of succinate to its major downstream product, fumarate. This photomixotrophic strain uses two proton symporters in opposite directions, glucose import requires a low or neutral pH for efficient consumption and the succinate transporter requires high pH in order to export the product to the media. Thus, it was determined that a fluctuating pH would be required for efficient succinate production. The results provide useful insights into the viability of expanding photomixotrophic production platforms to scale up chemical bioproduction.

2. Methods

2.1. Reagents

The following reagents were obtained from Research Products International (RPI): glucose, cycloheximide, gentamycin, spectinomycin, kanamycin, thiamine and IPTG. Phusion polymerase was purchased from New England Biolabs. All synthetic oligonucleotides were synthesized by Integrated DNA Technologies.

2.2. Plasmid construction

All plasmids and primers used in this study are listed in **Tables S1** and **S2**, respectively. The target genes and vector fragments used to construct plasmids were amplified using PCR with the primers and templates described in **Table S3**. The gene *ppc* was cloned from a codon optimized gene fragment purchased from Genewiz from Azenta Life Sciences. The resulting fragments were assembled by sequence and ligation-independent cloning (Jeong et al., 2012). All constructed plasmids were verified via Sanger sequencing.

2.3. Strain construction

Strains used in this study are listed in **Table 1**. Transformation and integration via double homologous recombination were performed as previously described (Golden et al., 1987). In brief, cells at $OD_{730} \sim 0.4$ were collected from 2 ml of culture by centrifugation, washed, and concentrated in 300 µl of BG-11 medium. After adding plasmid DNA (2 µg) to the concentrated cells, the tube was wrapped in foil and incubated overnight at 30 °C. Cells were plated on a BG-11-agar solid media containing appropriate antibiotics and incubated at 30 °C under constant light until colonies appear. Complete chromosomal segregation for the introduced fragments was achieved through propagation of multiple generations on selective agar plates. Correct recombinants were confirmed for double crossover and gene fidelity by PCR and Sanger sequencing.

2.4. Culture conditions

Unless otherwise specified, 7942 cells were cultured in BG-11 medium (Golden et al., 1987) with the addition of 50 mM NaHCO $_3$ without the addition of HEPES buffer. For production experiments, the production media was either 2x BG-11 or 5x BG-11, which were composed of doubled or quintupled 1x BG-11 medium component concentrations, respectively, with the exception of HEPES-KOH, which was excluded from all conditions, and the addition of glucose, NaHCO $_3$ (20 mM), IPTG (1 mM), thiamine (10 mg l $^{-1}$), and appropriate antibiotics. Cells were grown at 30 °C with rotary shaking (100 rpm) and light (80 µmol photons·m $^{-2}$ s $^{-1}$ in the PAR range) provided by 86 cm 20 W fluorescent tubes. Light intensity was measured using a PAR quantum flux meter (Model MQ-200, Apogee Instruments). Cell growth was monitored by

measuring OD_{730} in a Microtek Synergy H1 plate reader (BioTek). Antibiotics concentrations were as follows: cycloheximide (50 mg l⁻¹), spectinomycin (20 mg l⁻¹), kanamycin (20 mg l⁻¹), gentamycin (10 mg l⁻¹) and chloramphenicol (5 mg l⁻¹).

Prior to succinate production, colonies were inoculated in BG-11 medium containing 50 mM NaHCO₃ and appropriate antibiotics and grown photoautotrophically. Cells at the exponential growth phase were adjusted to an OD₇₃₀ of 0.5 in 10 ml BG-11 medium including 20 mM NaHCO₃ (unless otherwise stated), 1 mM IPTG, 10 mg l⁻¹ thiamine and appropriate antibiotics in 20 ml glass tubes with a height of 15 cm and a diameter of 1.5 cm. For highdensity production experiments, cells were adjusted to an OD₇₃₀ of 5.0 in 25 ml of 2x BG-11 or 5x BG-11 medium in 250 ml baffled glass flasks with a maximum circumference of 83 cm². Appropriate concentrations of glucose were added as required. Every 24 h, 10% of the culture volume was removed, the pH was adjusted to 7.0 with 3.6 N HCl, and the removed volume was replaced with production media containing 200 mM NaHCO₃ if bicarbonate was included for that experimental condition. For Fig. 4, cells were collected by centrifugation and resuspended with fresh production media on day 3 and resuspended at an OD₇₃₀ of 5.0 in production media on day 6. For Fig. 5, the cells were harvested by centrifugation and resuspended in fresh media at a target OD₇₃₀ of 5. For Fig. 7, the cultures were maintained at an alkaline pH, the sampling volume was replaced daily, and no cell harvesting, or resuspension was performed. For Fig. 8, 5x BG-11 was used and no cell harvesting was performed.

2.5. Genome sequencing

Photoautotrophically grown cultures at an approximate OD_{730} of 0.8 were collected via centrifugation (20,000 x g for 3 min) and genomic DNA was extracted using a phenol-chloroform and ethanol precipitation protocol, as previously described (Clerico et al., 2007). Purified genomic DNA was analyzed by nanodrop for purity and concentration, and then submitted to the UC San Diego IGM Genomics Center for standard Illimuna library preparation according to the manufacturer's instructions and sequencing using an Illumina NovaSeq 6000. Resulting sequence data for wild-type 7942 and Strain 2 were analyzed for SNPs with BreSeq (Deatherage and Barrick, 2014) using default parameters.

2.6. Quantification of extracellular metabolites

Glucose and succinate concentrations in culture supernatants were determined using a high-performance liquid chromatography (20A HPLC Shimadzu) equipped with a differential refractive detector 10A and an Agilent Hi-Plex H organic acid analysis column (Agilent). The mobile phase was 5 mM of H₂SO₄, maintained at a flow rate of 0.2 ml min⁻¹ at 55 °C for 18 min.

To prepare samples for HPLC analysis, 1 mL of cell culture was centrifuged at 20,000 x g for 10 min at 25 °C. 10 μ L of filtered culture supernatant was injected into the column for analysis.

Glucose consumption was determined by measuring glucose concentration in culture supernatants at each sampling point and subtracting it from the previous measurement.

Glucose concentration was also measured after resuspension in fresh media.

For analysis of Strain 14, fumarate and succinate were analyzed via UV-HPLC (UV at 210 nm) using an ACE C18-PFP 3 μ m particle size, 150x2.1mm Ultra-Inert HPLC Column (MacMod Analytical, Chadds Ford) with an isocratic method using 0.1% formic acid in MilliQ water, pH 3.5 on an Ultimate 3000 HPLC. Prior to HPLC analysis, 1 mL of cell culture was centrifuged at 20,000 x g for 3 min at room temperature and the supernatant was filtered through a 0.22 μ m filter. 10 μ L of filtered culture supernatant was injected into the column for analysis. Between samples, the column is washed with acetonitrile (ACN) for 8 min followed by a 5 min linear gradient back to the 0.1% formic acid solution and a 10 min equilibration step.

3. Results & Discussion

3.1 Installation of the glucose and succinate pathways to 7942

To utilize glucose, a glucose pathway that consists of three enzymes from *E. coli*; a galactose-proton symporter encoded by galP, a glucose-6-phosphate dehydrogenase encoded by zwf, and a 6-phosphogluconate dehydrogenase encoded by gnd was introduced to 7942 (**Fig. 1**) (Kanno et al., 2017). An isopropylthio- β -galactoside (IPTG)-inducible P_{LlacO1} (Till et al., 2020) was utilized to express galP-zwf-gnd (**Table 1**). The glucose pathway was observed in a previous study to enable a cyanobacterial strain to efficiently incorporate glucose into central carbon

metabolism via the oxidative branch of the pentose phosphate pathway. This pathway also improved the carbon fixing ability of the cyanobacterial strain by increasing the substrate pool for the CO₂ fixing enzyme, ribulose-1,5-bisphosphate carboxylase/oxygenase (RuBisCO) (Kanno et al., 2017). 7942 has an incomplete TCA cycle, thus the succinate semialdehyde shunt which includes kqd cloned from 7002 gDNA (Synpcc7002 A2770) and qabD cloned from E. coli MG1655 (hereafter, MG1655) gDNA encoding for an α -ketoglutarate decarboxylase (KGDH) and succinate semialdehyde dehydrogenase (SSDH), respectively, (P_{LlacO1}:kgd-gabD) was introduced to the strain with the glucose pathway, creating Strain 1 (Table 1). These variants of gabD and kqd were selected based off their reported activities and due to their successful use in producing succinate in 7942 in a previous study (Lan and Wei, 2016). Strain 1 was unable to produce succinate. However, Strain 2 (Table 1), which was provided by the Lan group (Lan and Wei, 2016) and has the same succinate semialdehyde shunt genes, was able to produce succinate photoautotrophically (75 ± 15.2 mg L⁻¹ in 5 days when induced with 1 mM IPTG under photoautotrophic conditions in 1x BG-11 without bicarbonate supplementation). Because the heterologous expression cassettes in Strains 1 and 2 are equivalent, we hypothesized that background mutations may exist between the two strains. Thus, the genomes of the wild type and Strain 2 were re-sequenced to determine any genetic differences. Three single nucleotide polymorphisms (SNPs) were present on the genome of Strain 2 as compared to the wild type strain in the loci Synpcc7942 0884 (elongation factor tu), Synpcc7942 1475 (sbtA), and Synpcc7942_1988 (conserved hypothetical). Based on the observed lack of production in Strain 1 and the SNPs present in Strain 2, Strain 2 was used for further modifications.

203

204

205

206

207

208

209

210

211

212

213

214

215

216

217

218

219

220

221

222

223

224

225

226

227

228

229

230

231

The glucose pathway was introduced into Strain 2, creating Strain 3 (**Table 1**). Strain 3 with and without bicarbonate produced 352 ± 40.1 mg L⁻¹ and 300 ± 20.4 mg L⁻¹ succinate, respectively, after 5 days, a 4 - 4.3 fold increase over photoautotrophic production (**Fig. 2a, Fig. S1**). In the production experiments, Strain 3 produced fumarate as a major side product. To remove fumarate production, *sdhB* on the chromosome of Strain 3 was deleted, resulting in Strain 4. Succinate dehydrogenase (SDH) is responsible for the conversion of succinate to fumarate, as well as the generation of electrons that ultimately impact the redox state of the

plastoquinone pool (Cooley and Vermaas, 2001; Sengupta et al., 2020; Zhao et al., 2016). Strain 4 with and without bicarbonate produced 516 \pm 48.4 mg L⁻¹ and 543 \pm 12.3 mg L⁻¹ succinate, respectively, and no fumarate was detected via HPLC after 5 days (**Fig. 2a**). However, the addition of bicarbonate inhibited growth of Strain 4 (**Fig. 2c**). Although growth inhibition occurred, the *sdhB* knockout was used for further study due to its benefit to specific productivity in experiments with bicarbonate present, $0.012 \pm 0.001 \text{ g L}^{-1} \text{ OD}_{730}^{-1} \text{ day}^{-1}$ for Strain 3 and $0.054 \pm 0.002 \text{ g L}^{-1} \text{ OD}_{730}^{-1} \text{ day}^{-1}$ for Strain 4 (**Fig. 2abc**). Because these strains have a mutation in *sbtA*, we hypothesize that the synthetic combination of this transporter mutation and a redox imbalance from an incomplete reductive branch of the TCA cycle causes the observed bicarbonate-dependent growth inhibition of Strain 4. Further studies are needed to elucidate the inhibition mechanisms.

3.2. Increased carbon flux toward the TCA cycle

We hypothesized that increased carbon flux from central metabolism to the TCA cycle would remedy the growth detriment with bicarbonate. The ppc gene from Corynebacterium glutamicum (hereafter, Cg) under P_{LlacO1} was introduced to Strain 4, creating Strain 5 (**Table 1**). Phosphoenol pyruvate carboxylase (PEPC) encoded by ppc converts phosphoenolpyruvate to oxaloacetate through reaction with bicarbonate, thus potentially impacting the bicarbonate-dependent growth defect (Chen et al., 2014). The Cg variant of ppc was chosen because Cg is a known glutamate overproducer and it has been hypothesized that enzymes related to the TCA cycle from Cg would have a higher activity (Chen et al., 2014; Lan and Wei, 2016). Strain 5 did not show the growth detriment present in Strain 4 in the presence of bicarbonate (**Fig. 2d**). Succinate production was also improved in Strain 5 (**Fig. 2a**). Strain 5 with and without bicarbonate produced 586 \pm 9.88 mg L⁻¹ and 388 \pm 55.0 mg L⁻¹ succinate, respectively, after 5 days (**Fig. 2a**).

To identify efficient PEPC for succinate production, additional strains were constructed with *ppc* from MG1655 and 7942 (Strains 6 and 7 respectively (**Table 1**)). Overexpression of *ppc* in MG1655 is a well-established method for regenerating TCA cycle intermediates via carboxylation of intracellular pools of phosphoenol pyruvate towards oxaloacetate and this

reaction catalyzed by PEPC is highly favorable among other anaplerotic reactions (De Mey et al., 2010; Lan and Wei, 2016). We hypothesized that this variant would enhance succinate production in 7942. Additionally, we hypothesized that overexpression of native 7942 *ppc* would achieve similar results. Indeed, Strain 7 with 7942 *ppc* produced more succinate than Strain 5 (**Fig. 3a**, **Fig. S2**). In contrast, Strain 6 with *ppc* from MG1655 did not produce detectable levels of succinate (**Fig. 3a**). The MG1655 PEPC is allosterically inhibited by aspartate and citrate which may be one reason for the observed lack of succinate production in Strain 6. Additionally, PEPC from different species can be sensitive or insensitive to regulation by various metabolites, such as cyclic-di-AMP, which may not be present at relevant concentrations in 7942 (Choi et al., 2017; Kai et al., 2003; Piazza et al., 2018). Thus Strain 7 was used for further modifications.

To identify an efficient citrate synthase (GLTA) for succinate production, Strains 8, 9, and 10 were constructed using variants of *gltA* from *Cg*, MG1655, and 7942 along with the 7942 *ppc* (**Table 1**). GLTA converts oxaloacetate to citrate. We hypothesized that the additional expression of *gltA* would increase the carbon flux toward succinate. Strain 8 produced similarly to Strain 7, while Strains 9 and 10 produced much less than Strains 7 and 8 (**Fig. 3b**, **Fig. S3**). These results suggest that *gltA* is not the rate-limiting step in these strains and that there may be a bottleneck in upstream metabolism, in fact, overexpression of *gltA* in Strains 9 and 10 likely overburdened the cell causing the observed decrease in production. Additionally, GLTA requires two substrates, acetyl-CoA and oxaloacetate, since overexpression of *ppc* likely competes for the available phosphoenolpyruvate substrate pool, acetyl-CoA pools may be depleted compared to oxaloacetate in Strains 8 through 10, therefore the limitation is substrate availability not availability of the free GLTA enzyme.

3.3. Deregulation of the CB cycle

We have previously shown that the deletion of *cp12* and the additional expression of *prk* improved CO₂ fixation, glucose utilization, and product formation (Kanno et al., 2017). Cp12 is a regulatory protein that represses two important enzymes of the CB cycle, glyceraldehyde-3-phosphate dehydrogenase (GAPDH) and phosphoribulokinase (PRK). PRK converts D-ribulose-5-

phosphate to D-ribulose-1,5-bisphosphate, which is a substrate of RuBisCO (Spreitzer and Salvucci, 2002; Stec, 2012). The cp12 gene was deleted and the prk gene was additionally expressed without or with ppc (7942) or ppc (7942)-gltA (Cg), creating Strains 11, 12, and 13 (**Table 1**). Strain 11, without the additional expression of ppc and gltA, produced 761 \pm 20.9 mg L⁻¹ succinate, nearly double that of Strain 3 which is identical to Strain 11 except for the deletion of cp12 and overexpression of prk (**Fig. 3c, Fig. S4**). Strain 12 with the additional expression of ppc (7942) produced similarly to Strain 11, suggesting PEPC is not the limiting step in this strain. Strain 13 with the additional expression of ppc (7942) and gltA (Cg) produced the highest titers of succinate at 950 \pm 25.0 mg L⁻¹ (**Fig. 3c**). The observable benefit of overexpressing gltA in the context of Strain 13 compared to the nonbeneficial overexpression observed in Strains 8 through 10 is likely due to the upstream bottleneck being removed, most likely caused by increasing flux through the CB cycle, allowing for an increase in acetyl-CoA pools. Thus, we used Strain 13 in the following experiments.

3.4. High cell density succinate production

We attempted to optimize production conditions using Strain 13. The production experiment started at OD_{730} ~5. 7942 generally cannot grow to the high OD_{730} s achieved in this study under photoautotrophic conditions due to density-dependent light deficiencies without condensing cell cultures, however, photomixotrophic conditions allow for this deficiency to be removed through sugar supplementation of metabolism (Kanno et al., 2017; McEwen et al., 2013). The media were replaced at day 3 and 6 to refresh sugar and medium content. At day 6, the OD_{730} was adjusted to 5 (**Fig. 4**). Under these conditions, Strain 13 produced 4.0 ± 0.20 g L⁻¹ in 8 days (**Fig. 4a**). However, the cells had an observable growth burden following centrifugation and cell harvesting at Day 3 and 6. Interestingly, succinate production and glucose consumption remained constant in spite of this growth inhibition or post-media replacement lag phase (**Fig. 4ab**). To test the effects of the media replacement on Strain 13, another experiment was carried out where the cells were harvested at day 3 and the OD_{730} was adjusted back to 5 (**Fig. 5**). The culture suffered from poor growth following centrifugation, suggesting that full media replacement by centrifugation was not optimal for these experiments (**Fig. 5**).

3.5. Photomixotrophic succinate production with pH fluctuations

317

318

319

320

321

322

323

324

325

326

327

328

329

330

331

332

333

334

335

336

337

338

339

340

341

342

343

344

345

Both the glucose and succinate transporters are proton symporters (Geertsma et al., 2015; Zheng et al., 2010). A low pH is required for efficient glucose import and a high pH is required for efficient succinate export. Because an alkaline pH was found to be beneficial for photoautotrophic succinate production (Lan and Wei, 2016), the pH for photomixotrophic production needs to shift between low and high or maintain a pH that works for both. The secretion of succinate and other diacids to the media was previously hypothesized to occur through a diacid transporter, encoded by SynPCC7942 0366, which is predicted to rely on a proton gradient similar to the mechanism of the glucose transporter, GALP (Geertsma et al., 2015; Lan and Wei, 2016). To test this hypothesis, we generated Strain 14 through transposon insertional knockout of SynPCC7942 0366 in Strain 2 (Table 1). HPLC analysis of the supernatant from production cultures of Strains 2 or 14 demonstrated that both succinate and fumarate secretion are greatly reduced upon knockout of SynPCC7942_0366, supporting this gene's role in encoding a transporter (Fig. 6). GALP being a proton symporter uses a proton from the media to transport glucose across the bacterial membrane, therefore a neutral or acidic pH in the media is ideal for efficient sugar consumption (Zheng et al., 2010). First, we performed a high-density experiment wherein pH was maintained at alkaline levels instead of being adjusted back to a neutral pH daily (Fig. 7). The medium pH steadily increases as CO₂ in bicarbonate is fixed, resulting in the evolution of hydroxide. When succinate is not being produced, pH increases to ~10.5, which was shown to be a beneficial pH for photoautotrophic succinate production (Lan and Wei, 2016). When succinate was being produced, the medium was acidified to a pH of approximately 9.5, where pH equilibrated even as succinate continued to be produced (Fig. 7). Strain 13 under this condition produced 2.8 ± 0.056 g L⁻¹ succinate in 7 days (Fig. 7a), which was lower than that with pH adjustment where 4.0 ± 0.20 g L⁻¹ succinate was produced (Fig. 4). Glucose consumption was diminished under the alkaline conditions (day 0 to day 3, 3.5 \pm 0.062 g L⁻¹ d ⁻¹ and day 3 to day 7, 2.3 \pm 0.11 g L⁻¹ d ⁻¹, **Fig. 7b**) compared to glucose consumption prior to centrifugation on day 3 in a previous high-density experiment (4.1 ± 0.23 g L⁻¹ d ⁻¹, Fig. 4b). We hypothesize that the decrease in glucose consumption resulted in lower succinate titers. The previous experiment with pH adjustment (Fig. 4) was conducted in

2x BG-11 and the cultures were centrifuged. We hypothesized that 5x BG-11 would be beneficial for high density experiments. Since succinate production and glucose consumption were both diminished in the 5x BG-11 condition compared to 2x BG-11, it became necessary to investigate if the alkaline conditions were at fault for the diminished metrics as we hypothesized. It should be noted that changes in pH can cause variation in many factors ranging from enzyme kinetics to CO_2 fixation rates and growth. Studies suggest that 7942 favors alkaline conditions for photoautotrophic growth and protein production (Mangan et al., 2016; Martinho de Brito et al., 2022). Further study is required to determine how photomixotrophic metabolism is affected under different pH conditions in 7942. However, intracellular pH is generally stable in 7942, ranging only from 7.16 ± 0.03 to 7.55 ± 0.02 in media with pH ranging from 5 to 10 (Ritchie, 1991).

Given these results, we chose to focus on enhancing glucose import by adjusting the medium pH to 7 daily since it is known that the GALP transporter functions best at acidic or neutral medium pH (Zheng et al., 2010). Bicarbonate in the media offers the ability to increase pH with hydroxide evolution. The sensitivity to bicarbonate found in Strain 4 was removed by additionally expressing ppc (Fig. 2ad), making Strain 13 amenable to bicarbonate-dependent pH adjustments. Additionally, succinate acidifies the culture media upon production. To investigate the pH effects of both bicarbonate and succinate, a production experiment was started at pH 7 and the pH was adjusted back to pH 7 every day (Fig. 8). In this experiment, pH was allowed to fluctuate to alkaline levels due to the evolution of hydroxide from bicarbonate and was adjusted back to neutral levels daily. The pH was measured prior to adjustment and was determined to be indicative of succinate production. By day 1, minimal succinate production had occurred, and pH remained at 10.5 (Fig. 8c). The highest succinate productivity rates were observed from day 2-5, and subsequently pH was lower (pH ~8.5) prior to adjustment during that time due to the produced succinate acidifying the medium (Fig. 8ac). By days 9-10 succinate productivity decreased, therefore, pH of the cultures was more alkaline prior to adjustment (pH ~9.5) (Fig. 8ac). Glucose consumption also correlated well with succinate production and decreased pH; glucose consumption was highest $(3.9 \pm 0.26 \text{ g L}^{-1}\text{d}^{-1})$ during days 2-5 where succinate production was decreasing medium pH to more neutral levels (pH ~8.5

prior to adjustment) (**Fig. 8b**). Glucose consumption was lower ($2.2 \pm 0.59 \text{ g L}^{-1}\text{d}^{-1}$) on days 9-10 when the medium was more alkaline (**Fig. 8b**). Increased succinate production correlated with exponential growth (**Fig. 8d**) while decreased rates correlated with a stationary phase of growth. Strain 13 under this condition produced $5.0 \pm 0.41 \text{ g L}^{-1}$ succinate and efficiently consumed glucose ($3.5 \pm 0.44 \text{ g L}^{-1} \text{d}^{-1}$) over the entire time course.

4. Conclusion

We improved glucose assimilation and succinate production through gene knockout and overexpression. The pH of the media was observed to be important to both the production of succinate and the consumption of glucose. We investigated various production conditions, our findings in this study show that a fluctuating pH enhances succinate production compared to a stable high pH. Further studies are needed to elucidate whether these results are due to the proton symporters involved in glucose import and succinate export, or to metabolic changes under these various pH conditions. We also hypothesize that a fluctuating pH is natural in an outdoor growth environment due to the diel cycle as CO₂ fixation rates naturally oscillate. This natural oscillation in medium pH was mimicked in the laboratory scale cultures and we determined that succinate can be produced under fluctuating pH conditions. Research into the effects of pH on photomixotrophic production of chemical commodities warrants further exploration to determine the next steps towards optimizing a large scale outdoor cyanobacterial cultivation process. Additionally, this study demonstrated that photomixotrophy in cyanobacteria can be applied to other production systems and is generally an effective way for enhancing production of valuable chemical commodities.

Acknowledgements

This work was supported by the Department of Energy (DE-EE0008491) and the National Science Foundation (CBET-1902014). We thank Ethan Lan (NYCU, Taiwan) for providing Strain 2. This publication includes data generated at the UC San Diego IGM Genomics Center utilizing an

402 Illumina NovaSeq 6000 that was purchased with funding from a National Institutes of Health 403 SIG grant (#S10 OD026929). 404 **Author contributions** T.T., R.P., S.M., R.S., and S.A. designed research; T.T., M.T., and R.S. performed the experiments; 405 T.T., M.T., R.P., R.S., and S.A. analyzed data; T.T., R.S., and S.A. wrote the manuscript. 406 407 **Competing interests** 408 The authors declare no competing interests. 409 References 410 411 Ahn, J.H., Jang, Y.S., Lee, S.Y., 2016. Production of succinic acid by metabolically engineered microorganisms. Curr. Opin. Biotechnol. 42, 54–66. 412 https://doi.org/10.1016/j.copbio.2016.02.034 413 414 Berla, B.M., Saha, R., Immethun, C.M., Maranas, C.D., Moon, T.S., Pakrasi, H.B., 2013. Synthetic biology of cyanobacteria: Unique challenges and opportunities. Front. Microbiol. 4, 1–14. 415 https://doi.org/10.3389/fmicb.2013.00246 416 417 Chen, Z., Bommareddy, R.R., Frank, D., Rappert, S., Zeng, A.P., 2014. Deregulation of feedback 418 inhibition of phosphoenolpyruvate carboxylase for improved lysine production in Corynebacterium glutamicum. Appl. Environ. Microbiol. 80, 1388–1393. 419 420 https://doi.org/10.1128/AEM.03535-13 Choi, P.H., Vu, T.M.N., Pham, H.T., Woodward, J.J., Turner, M.S., Tong, L., 2017. Structural and 421 functional studies of pyruvate carboxylase regulation by cyclic di-AMP in lactic acid 422 bacteria. Proc. Natl. Acad. Sci. U. S. A. 114, E7226–E7235. 423 https://doi.org/10.1073/pnas.1704756114 424 425 Clerico, E.M., Ditty, J.L., Golden, S.S., 2007. Specialized techniques for site-directed mutagenesis in cyanobacteria. Methods Mol. Biol. 362, 155–171. https://doi.org/10.1007/978-1-59745-426 427 257-1 11

428 Cooley, J.W., Vermaas, W.F.J., 2001. Succinate dehydrogenase and other respiratory pathways 429 in thylakoid membranes of Synechocystis sp. strain PCC 6803: Capacity comparisons and 430 physiological function. J. Bacteriol. 183, 4251–4258. https://doi.org/10.1128/JB.183.14.4251-4258.2001 431 432 Cozier, M., 2014. Business highlights: Collaboration: Bigger and beta. Biofuels, Bioprod. 433 Biorefining 8, 743. https://doi.org/10.1002/BBB 434 De Mey, M., Lequeux, G.J., Beauprez, J.J., Maertens, J., Waegeman, H.J., Van Bogaert, I.N., 435 Foulquié-Moreno, M.R., Charlier, D., Soetaert, W.K., Vanrolleghem, P.A., Vandamme, E.J., 436 2010. Transient metabolic modeling of Escherichia coli MG1655 and MG1655 ΔackA-pta, $\Delta poxB \ \Delta pppc$ ppc-p37 for recombinant β -galactosidase production. J. Ind. Microbiol. 437 Biotechnol. 37, 793-803. https://doi.org/10.1007/s10295-010-0724-7 438 439 Deatherage, D.E., Barrick, J.E., 2014. Identification of mutations in laboratory-evolved microbes 440 from next-generation sequencing data using breseq. Methods Mol. Biol. 1151, 165–188. 441 https://doi.org/10.1007/978-1-4939-0554-6 12 442 François, J.M., Lachaux, C., Morin, N., 2020. Synthetic Biology Applied to Carbon Conservative 443 and Carbon Dioxide Recycling Pathways. Front. Bioeng. Biotechnol. 7, 1–16. https://doi.org/10.3389/fbioe.2019.00446 444 445 Geertsma, E.R., Chang, Y.N., Shaik, F.R., Neldner, Y., Pardon, E., Steyaert, J., Dutzler, R., 2015. 446 Structure of a prokaryotic fumarate transporter reveals the architecture of the SLC26 447 family. Nat. Struct. Mol. Biol. 22, 803-808. https://doi.org/10.1038/nsmb.3091 Golden, S.S., Brusslan, J., Haselkorn, R., 1987. Genetic Engineering of the Cyanobacterial 448 449 Chromosome. Methods Enzymol. 153, 215-231. https://doi.org/10.1016/0076-450 6879(87)53055-5 451 Hasunuma, T., Matsuda, M., Kato, Y., Vavricka, C.J., Kondo, A., 2018. Temperature enhanced 452 succinate production concurrent with increased central metabolism turnover in the cyanobacterium Synechocystis sp. PCC 6803. Metab. Eng. 48, 109–120. 453 https://doi.org/10.1016/j.ymben.2018.05.013 454

- 455 lijima, H., Watanabe, A., Sukigara, H., Iwazumi, K., Shirai, T., 2021. Four-carbon dicarboxylic acid
- 456 production through the reductive branch of the open cyanobacterial tricarboxylic acid
- 457 cycle in *Synechocystis* sp. PCC 6803. Metab. Eng. 65, 88–98.
- 458 https://doi.org/10.1016/j.ymben.2021.03.007
- 459 Jeong, J.Y., Yim, H.S., Ryu, J.Y., Lee, H.S., Lee, J.H., Seen, D.S., Kang, S.G., 2012. One-step
- sequence-and ligation-independent cloning as a rapid and versatile cloning method for
- functional genomics Studies. Appl. Environ. Microbiol. 78, 5440–5443.
- 462 https://doi.org/10.1128/AEM.00844-12
- 463 Kai, Y., Matsumura, H., Izui, K., 2003. Phosphoenolpyruvate carboxylase: Three-dimensional
- structure and molecular mechanisms. Arch. Biochem. Biophys. 414, 170–179.
- 465 https://doi.org/10.1016/S0003-9861(03)00170-X
- Kanno, M., Carroll, A.L., Atsumi, S., 2017. Global metabolic rewiring for improved CO₂ fixation
- and chemical production in cyanobacteria. Nat. Commun. 8, 1–11.
- 468 https://doi.org/10.1038/ncomms14724
- Lai, M.J., Tsai, J.C., Lan, E.I., 2022. CRISPRi-enhanced direct photosynthetic conversion of carbon
- dioxide to succinic acid by metabolically engineered cyanobacteria. Bioresour. Technol.
- 471 366, 128131. https://doi.org/10.1016/j.biortech.2022.128131
- Lan, E.I., Wei, C.T., 2016. Metabolic engineering of cyanobacteria for the photosynthetic
- 473 production of succinate. Metab. Eng. 38, 483–493.
- 474 https://doi.org/10.1016/j.ymben.2016.10.014
- Lee, J.W., Kim, H.U., Choi, S., Yi, J., Lee, S.Y., 2011. Microbial production of building block
- chemicals and polymers. Curr. Opin. Biotechnol. 22, 758–767.
- 477 https://doi.org/10.1016/j.copbio.2011.02.011
- 478 Li, Q., Huang, B., Wu, H., Li, Z., Ye, Q., 2017. Efficient anaerobic production of succinate from
- glycerol in engineered Escherichia coli by using dual carbon sources and limiting oxygen
- supply in preceding aerobic culture. Bioresour. Technol. 231, 75–84.
- 481 https://doi.org/10.1016/j.biortech.2017.01.051

482 Mangan, N.M., Flamholz, A., Hood, R.D., Milo, R., Savage, D.F., 2016. pH determines the 483 energetic efficiency of the cyanobacterial CO₂ concentrating mechanism. Proc. Natl. Acad. 484 Sci. U. S. A. 113, E5354–E5362. https://doi.org/10.1073/pnas.1525145113 485 Martinho de Brito, M., Bundeleva, I., Marin, F., Vennin, E., Wilmotte, A., Plasseraud, L., Visscher, 486 P.T., 2022. Effect of Culture pH on Properties of Exopolymeric Substances from Synechococcus PCC7942: Implications for Carbonate Precipitation. Geosci. 12, 210. 487 488 https://doi.org/10.3390/geosciences12050210 489 McEwen, J.T., Machado, I.M.P., Connor, M.R., Atsumi, S., 2013. Engineering Synechococcus 490 elongatus PCC 7942 for continuous growth under diurnal conditions. Appl. Environ. Microbiol. 79, 1668–1675. https://doi.org/10.1128/AEM.03326-12 491 492 Newark, 2020. Global Succinic Acid Market is Expected to Reach USD 218.14 [WWW 493 Document]. URL https://www.globenewswire.com/news-494 release/2020/01/30/1977366/0/en/Global-Succinic-Acid-Market-is-Expected-to-Reach-495 USD-218-14-Million-by-2025-Fior-Markets.html (accessed 3.21.23). 496 Nozzi, N.E., Oliver, J.W.K., Atsumi, S., 2013. Cyanobacteria as a Platform for Biofuel Production. 497 Front. Bioeng. Biotechnol. 1, 1–6. https://doi.org/10.3389/fbioe.2013.00007 Piazza, I., Kochanowski, K., Cappelletti, V., Fuhrer, T., Noor, E., Sauer, U., Picotti, P., 2018. A Map 498 499 of Protein-Metabolite Interactions Reveals Principles of Chemical Communication. Cell 500 172, 358-372.e23. https://doi.org/10.1016/j.cell.2017.12.006 Ritchie, R.J., 1991. Membrane Potential and pH Control in the Cyanobacterium Synechococcus 501 R-2 (Anacystis nidulans) PCC 7942. J. Plant Physiol. 137, 409–418. 502 503 https://doi.org/10.1016/S0176-1617(11)80309-3 Sengupta, S., Jaiswal, D., Sengupta, A., Shah, S., Gadagkar, S., Wangikar, P.P., 2020. Metabolic 504 505 engineering of a fast-growing cyanobacterium Synechococcus elongatus PCC 11801 for 506 photoautotrophic production of succinic acid. Biotechnol. Biofuels 13, 1–18. https://doi.org/10.1186/s13068-020-01727-7 507

| 508 | Sheldon, R.A., 2014. Green and sustainable manufacture of chemicals from biomass: State of |
|-----|---|
| 509 | the art. Green Chem. 16, 950–963. https://doi.org/10.1039/c3gc41935e |
| 510 | Spreitzer, R.J., Salvucci, M.E., 2002. Rubisco: Structure, regulatory interactions, and possibilities |
| 511 | for a better enzyme. Annu. Rev. Plant Biol. 53, 449–475. |
| 512 | https://doi.org/10.1146/annurev.arplant.53.100301.135233 |
| 513 | Stec, B., 2012. Structural mechanism of RuBisCO activation by carbamylation of the active site |
| 514 | lysine. Proc. Natl. Acad. Sci. U. S. A. 109, 18785–18790. |
| 515 | https://doi.org/10.1073/pnas.1210754109 |
| 516 | Steinhauser, D., Fernie, A.R., Araújo, W.L., 2012. Unusual cyanobacterial TCA cycles: Not broken |
| 517 | just different. Trends Plant Sci. 17, 503–509. https://doi.org/10.1016/j.tplants.2012.05.005 |
| 518 | Stephens, S., Mahadevan, R., Allen, D.G., 2021. Engineering Photosynthetic Bioprocesses for |
| 519 | Sustainable Chemical Production: A Review. Front. Bioeng. Biotechnol. 8, 1–15. |
| 520 | https://doi.org/10.3389/fbioe.2020.610723 |
| 521 | Till, P., Toepel, J., Bühler, B., Mach, R.L., Mach-Aigner, A.R., 2020. Regulatory systems for gene |
| 522 | expression control in cyanobacteria. Appl. Microbiol. Biotechnol. 104, 1977–1991. |
| 523 | https://doi.org/10.1007/s00253-019-10344-w |
| 524 | Uprety, D.C., Reddy, V.R., Mura, J.D., 2019. Historical Analysis of Climate Change and |
| 525 | Agriculture, Climate Change and Agriculture. https://doi.org/10.1007/978-981-13-2014- |
| 526 | 9_2 |
| 527 | Zhao, Y., Wang, C.S., Li, F.F., Liu, Z.N., Zhao, G.R., 2016. Targeted optimization of central carbon |
| 528 | metabolism for engineering succinate production in Escherichia coli. BMC Biotechnol. 16, |
| 529 | 52. https://doi.org/10.1186/s12896-016-0284-7 |
| 530 | Zheng, H., Taraska, J., Merz, A.J., Gonen, T., 2010. The Prototypical H+/Galactose Symporter |
| 531 | GalP Assembles into Functional Trimers. J. Mol. Biol. 396, 593–601. |
| 532 | https://doi.org/10.1016/j.jmb.2009.12.010 |

Table 1 List of strains used in this study

| Strai | Key genotype | Ref | |
|-------|---|------------------------|--|
| no. | кеу веногуре | Kei | |
| 1 | NSI:: P_{trc} : $galP$ - zwf - gnd ; Spec ^R NSIII:: P_{trc} : $gabD$ (MG1655)- kgd (7002); Gent ^R | This work | |
| 2 | NSI:: <i>P_{trc}:gabD</i> (MG1655)- <i>kgd</i> (7002); Spec ^R | (Lan and Wei, 2016) | |
| 3 | 2 + NSII:: <i>P_{trc}:galP-zwf-gnd</i> (MG1655); Kan ^R | This work | |
| 4 | 3 + sdhB::Gent ^R | This work | |
| 5 | $3 + sdhB::P_{LlacO1}:ppc (Cg); Gent^R$ | This work | |
| 6 | 3 + sdhB::P _{LlacO1} :ppc (MG1655); Gent ^R | This work | |
| 7 | 3 + <i>sdhB</i> :: <i>P</i> _{LlacO1} : <i>ppc</i> (7942); Gent ^R | This work | |
| 8 | $3 + sdhB::P_{LlacO1}:ppc (7942)-gltA (Cg); Gent^{R}$ | This work | |
| 9 | 3 + sdhB::P _{LlacO1} :ppc (7942)–gltA (MG1655); Gent ^R | This work | |
| 10 | 3 + sdhB::P _{LlacO1} :ppc (7942)–gltA (7942); Gent ^R | This work | |
| 11 | 2 + $cp12$:: P_{LlacO1} : $prk P_{trc}$: $galP$ - zwf - gnd ; Kan^R | This work | |
| 12 | 11 + sdhB::P _{LlacO1} :ppc (7942); Gent ^R | This work | |
| 13 | 11 + $sdhB::P_{LlacO1}:ppc$ (7942)– $gltA$ (Cg); $Gent^{R}$ | This work | |
| 14 | 2 + Synpcc7942_0366::Tn5; Kan ^R | This work | |

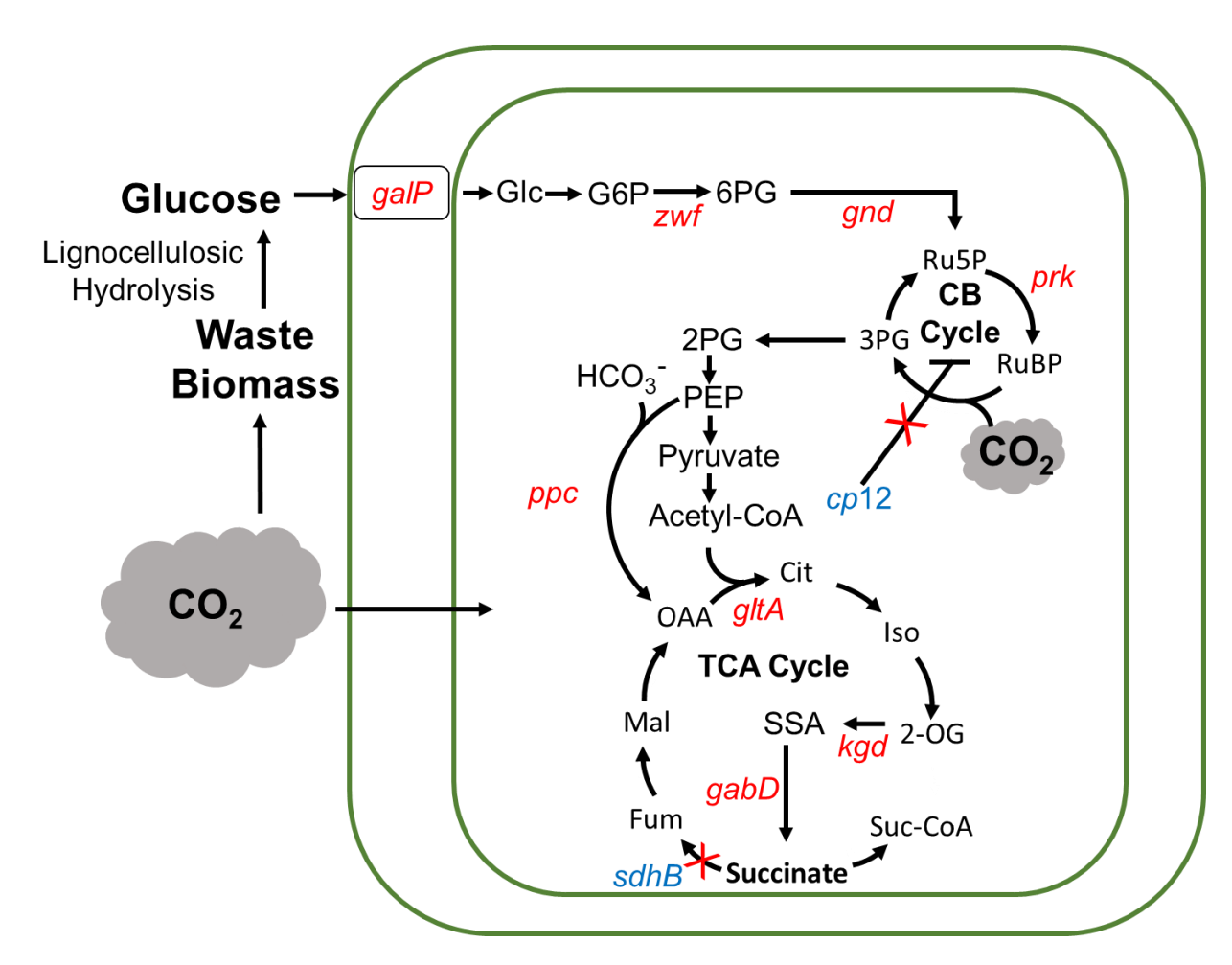
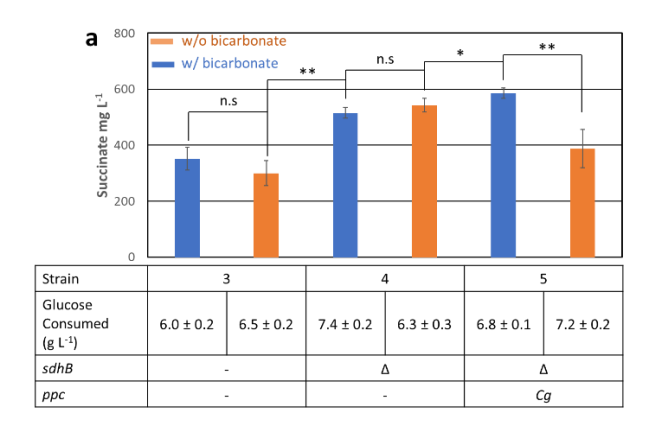


Figure 1. Photomixotrophic Succinate Production Pathway.

Genes in red are overexpressed and genes in blue are deleted in this study. GalP, galactose-proton symporter; Zwf, G6P dehydrogenase; Gnd, 6PG dehydrogenase; G6P, glucose-6-phosphate; 6PG, 6-phosphogluconate; Prk, phophoribulokinase; RuBP, ribulose-1,5-bisphosphate; Ru5P, ribulose-5-phosphate; Cp12, a regulatory protein of the CB cycle; 3PG, 3-phosphoglycerate; 2PG, 2-phosphoglycerate; PEP, phosphoenolpyruvate; PEPC encoded by *ppc*, phosphoenolpyruvate carboxylase; Cit, citrate; GLTA encoded by *gltA*, citrate synthase; Iso, isocitrate; 2OG, 2-oxoglutarate; KGDH encoded by *kgd*, oxoglutarate dehydrogenase; SSDH encoded by *gabD*, succinate semialdehyde dehydrogenase; Suc-CoA, succinyl-CoA; SdhB, succinate dehydrogenase subunit B; Fum, fumarate; Mal, malate; OAA, oxaloacetate.



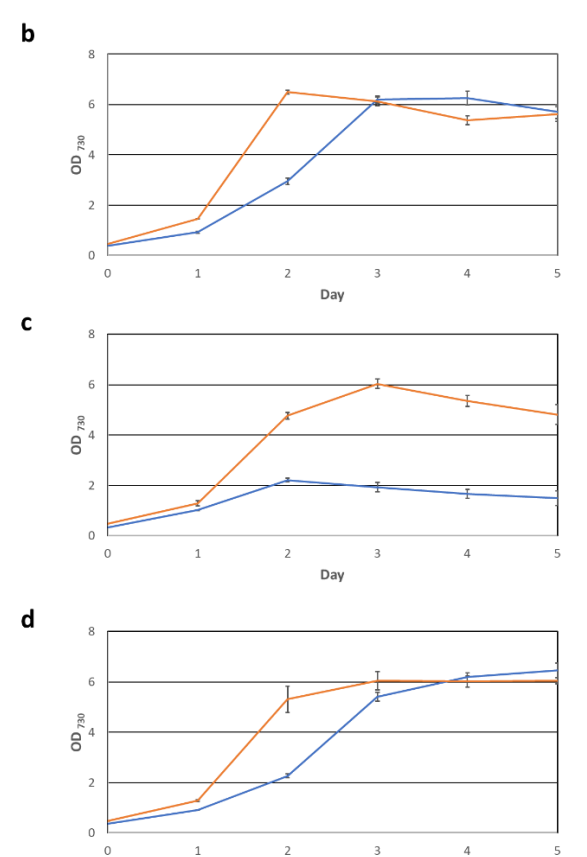


Figure 2. Photomixotrophic succinate production and growth of strains 3, 4, and 5. a) production b-d) Growth of Strains 3, 4, and 5 (**Table 1**) with (blue) and without (orange) 20 mM bicarbonate. Error bars indicate s.d. (n = 3 biological replicates). For significance calculations, n.s represents no significant difference P > 0.05, (*) represents $P \le 0.05$, (**) represents $P \le 0.01$, (***) $P \le 0.001$ using an unpaired t-test. Experiment was performed in 1x BG-11 with 10 g L⁻¹ glucose.

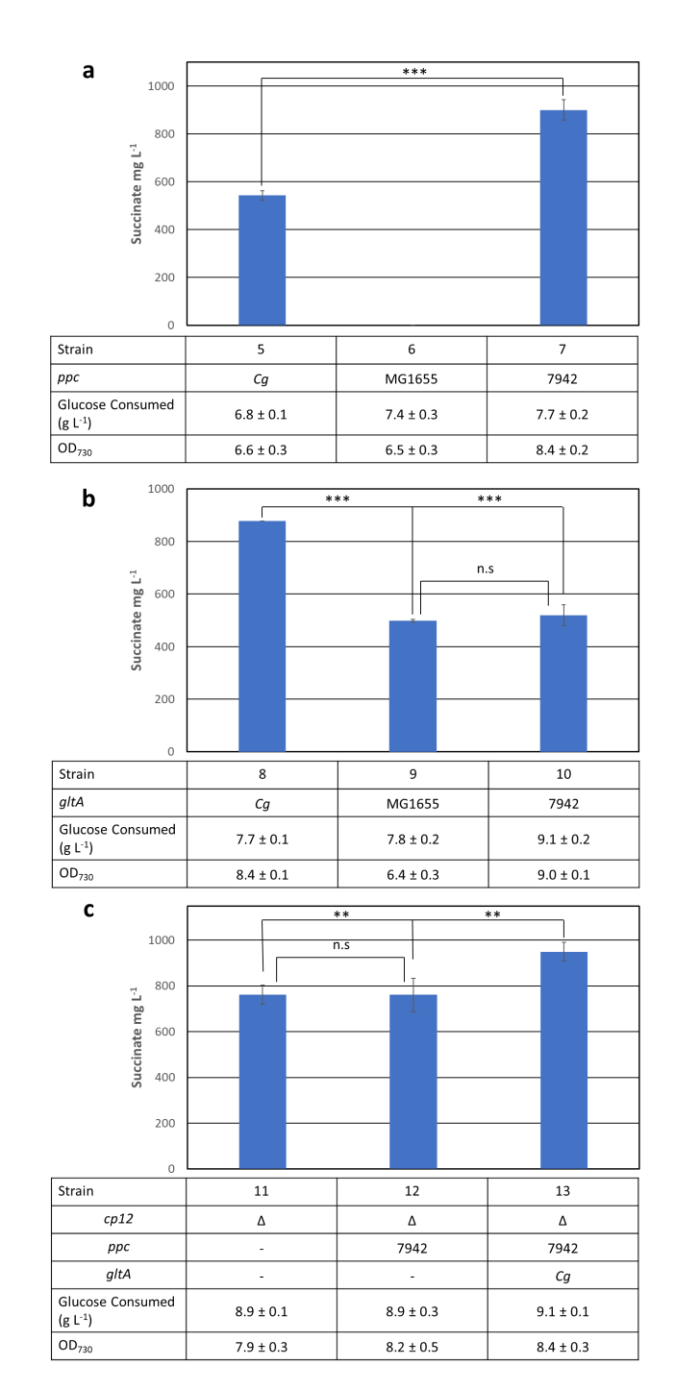


Figure 3. Low density photomixotrophic succinate production of strains 5-13.

a) Production of succinate in strains 5, 6, and 7 (**Table 1**) to evaluate optimal *ppc* variant. b) Production of succinate in Strains 8, 9 and 10 (**Table 1**) to evaluate optimal *gltA* variant. c) Production of succinate in Strains 11, 12 and 13 (**Table 1**). Each strain was cultivated in BG-11 supplemented with 20 mM sodium bicarbonate and 10g L⁻¹ glucose. Appropriate antibiotics and inducers were also added. Error bars indicate standard deviation (n = 3 biological replicates). For significance calculations, n.s represents no significant difference P > 0.05, (*) represents $P \le 0.05$, (**) represents $P \le 0.01$, (***) $P \le 0.001$ using an unpaired t-test.

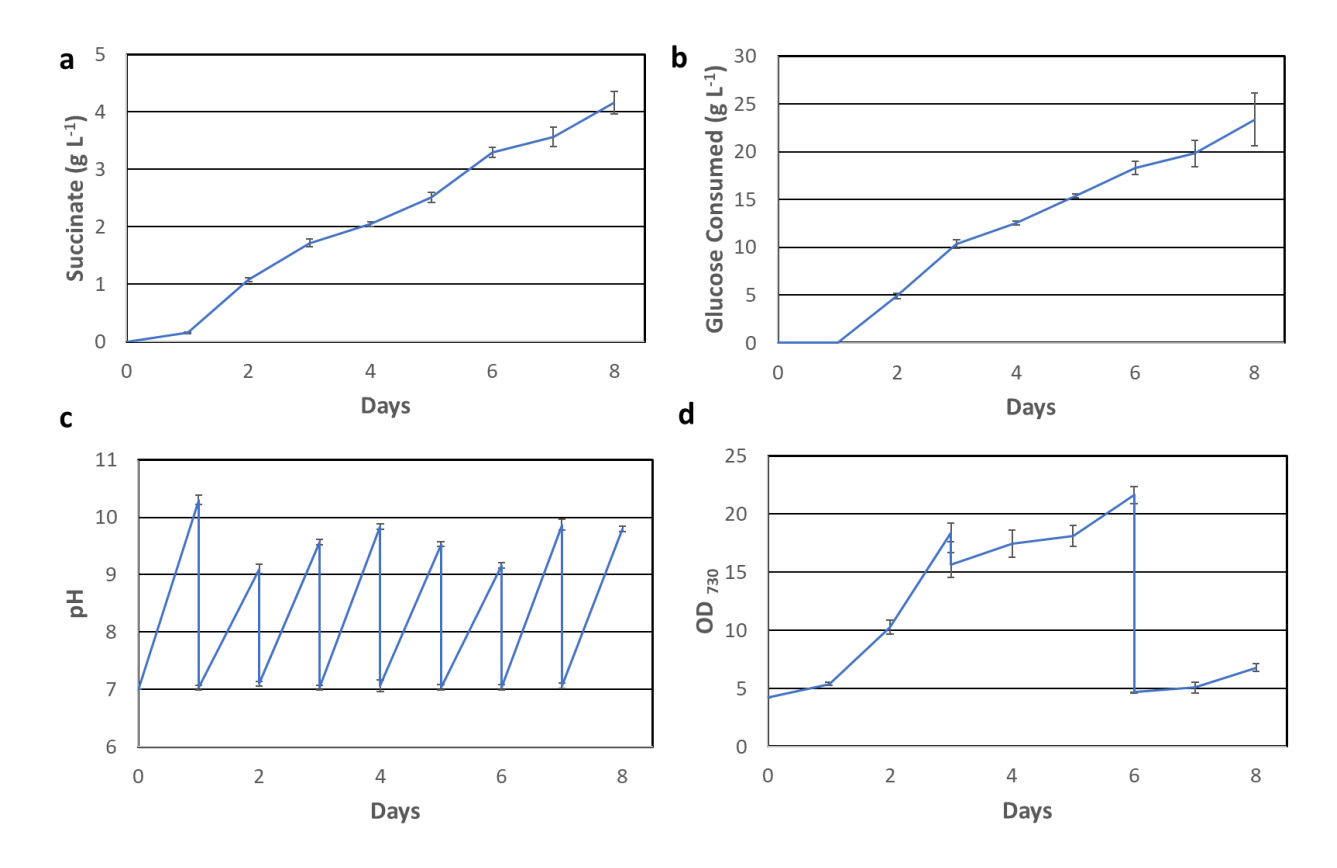


Figure 4. Effects of media replacement on Strain 13

a) Succinate production. b) Glucose consumed over the time course of the experiment. c) pH changes over time. pH was adjusted back to 7 every 24 hours; pH was recorded prior to adjustment. Both pH measurements prior to adjustment and post adjustment are plotted. d) OD_{730} on day 3, cells were collected by centrifugation and resuspended in fresh production media. On day 6, cells were collected by centrifugation and resuspended at an OD_{730} 5 in fresh production media. Error bars indicate s.d. (n = 3 biological replicates). Experiment was performed in 2x BG-11 with 40 g L⁻¹ glucose and 20mM bicarbonate.

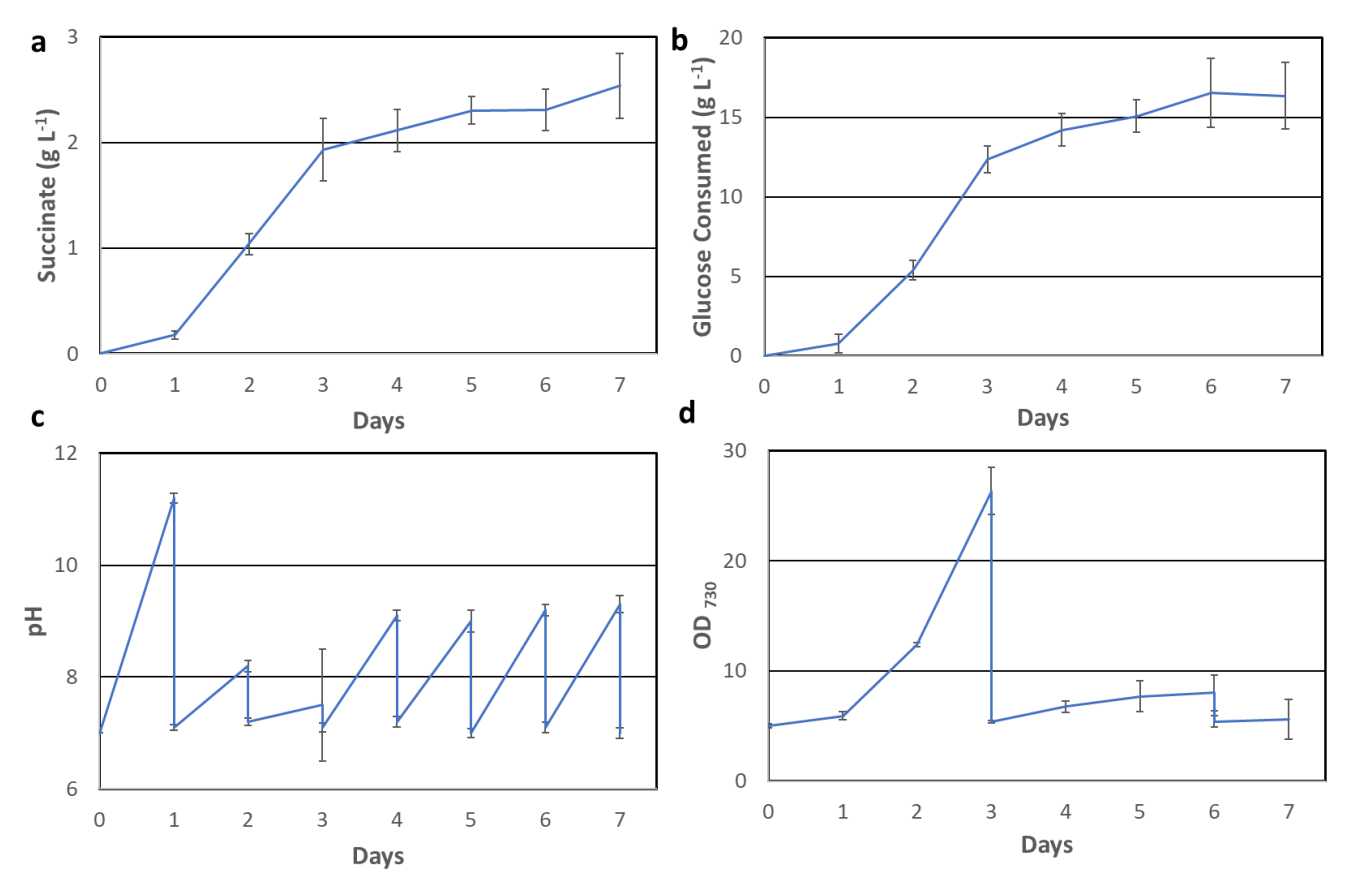


Figure 5. High density succinate production in Strain 13 with centrifugation and media replacement in 2x BG-11

a) Succinate production. b) Glucose consumed over the time course of the experiment. c) pH changes over time. pH was adjusted back to 7 every 24 hours; pH was recorded prior to adjustment. Both pH measurements prior to adjustment and post adjustment are plotted. d) OD_{730} on day 3, cells were collected by centrifugation, resuspended, and adjusted down to an OD_{730} of 5 in fresh production media. On day 6, cells were collected by centrifugation and resuspended in fresh production media. Error bars indicate s.d. (n = 3 biological replicates). Experiment was performed in 2x BG-11 with 40 g L⁻¹ glucose and 20mM bicarbonate.

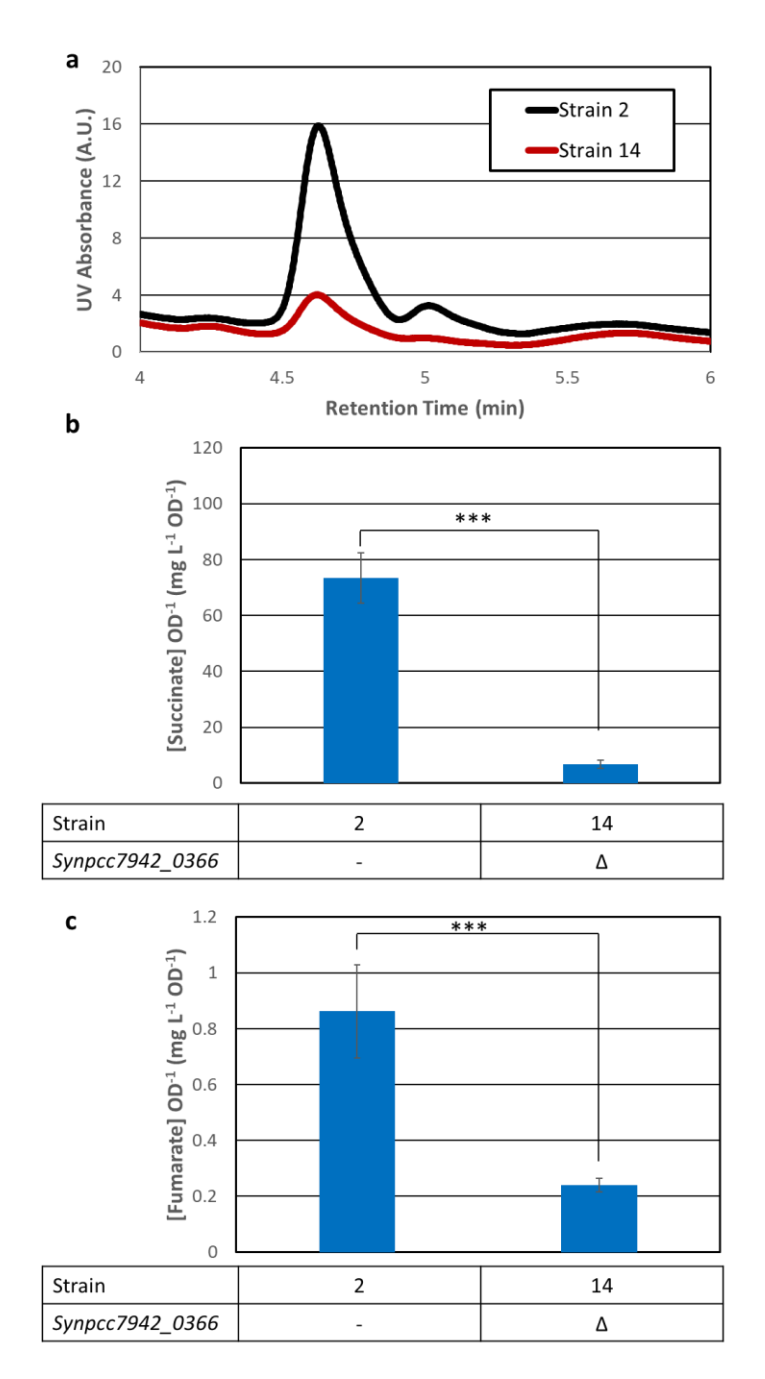


Figure 6. Inhibition of secretion of fumarate and succinate upon knockout of Synpcc7942 0366.

a) HPLC-UV retention traces of supernatant samples from production cultures of Strains 2 (black) and 14 (red). Spike-ins of pure fumarate or succinate demonstrate that fumarate runs at a retention time of 4.65 min and succinate runs at 5.0 min. b) Specific titer of succinate in strains 2 and 14. c) Specific titer of fumarate in strains 2 and 14. For significance calculations, n.s represents no significant difference P > 0.05, (*) represents $P \le 0.05$, (**) represents $P \le 0.01$, (***) $P \le 0.001$ using an unpaired t-test.

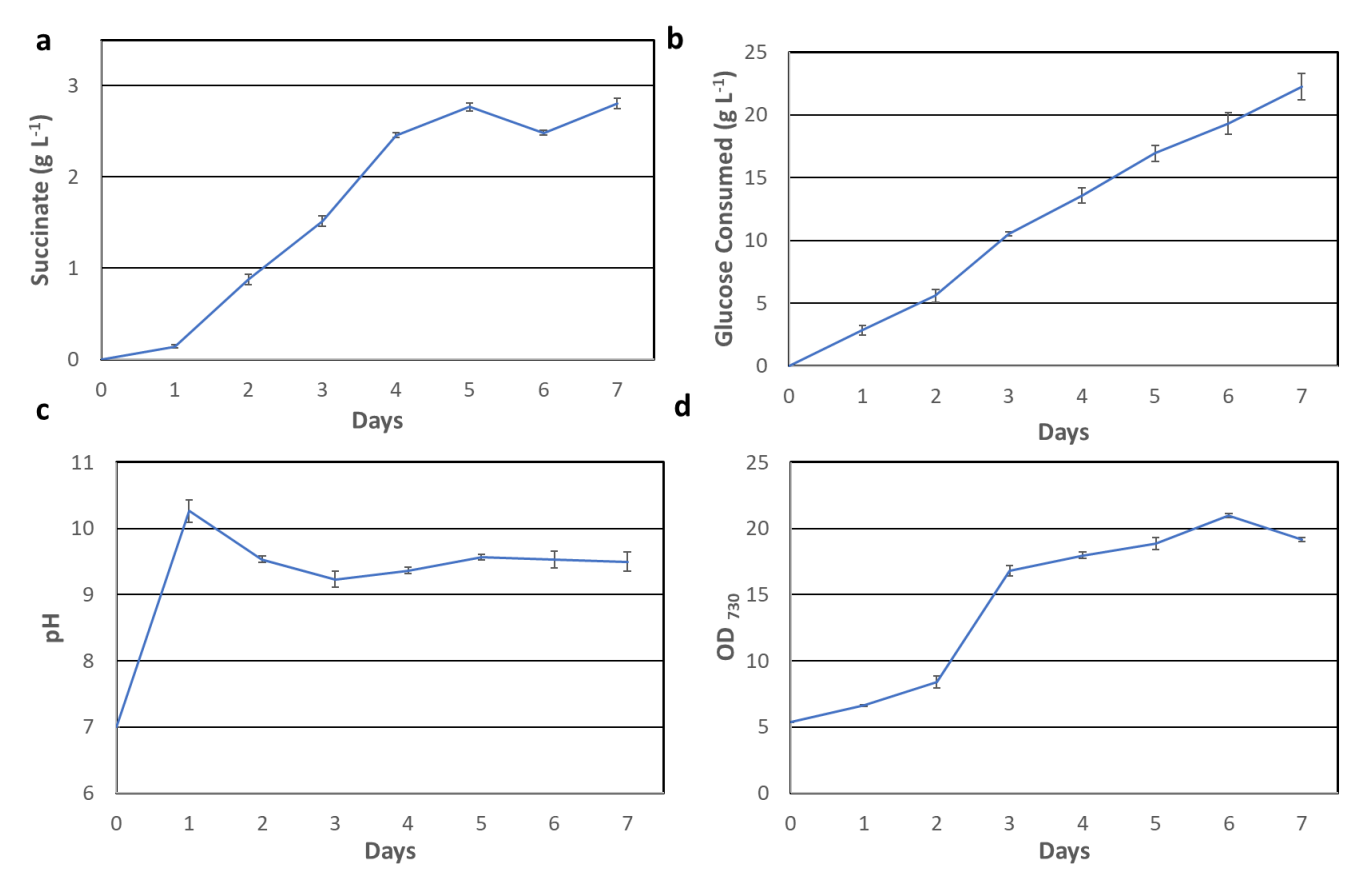


Figure 7. High density succinate experiment in strain 13 at high pH in 5x BG-11 a) Succinate production. b) Glucose consumed over the time course of the experiment. c) pH over time. d) OD_{730} . Error bars indicate s.d. (n = 3 biological replicates). Experiment was performed in 5x BG-11 with 40 g L⁻¹ glucose and 20 mM bicarbonate.

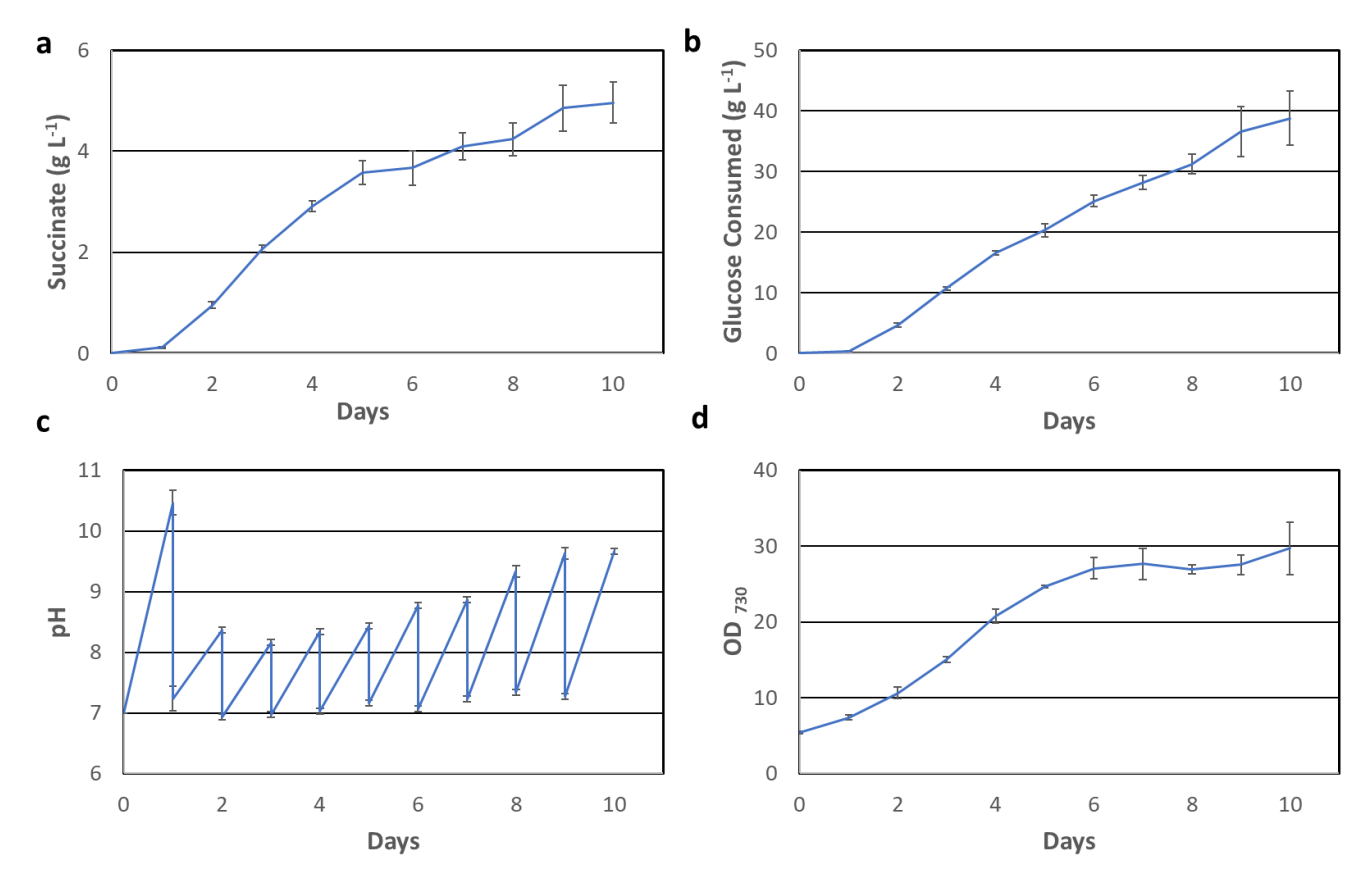


Figure 8. High density photomixotrophic succinate production in strain 13 with fluctuating pH a) Succinate production. b) Glucose consumed over the time course of the experiment. c) pH changes over time. pH was adjusted back to 7 every 24 hours; pH was recorded prior to adjustment. Both pH measurements prior to adjustment and post adjustment are plotted. d) OD_{730} . Error bars indicate s.d. (n = 3 biological replicates). Experiment was performed in 5x BG-11 with 40 g L-1 glucose and 20 mM bicarbonate.